


Catalytic reduction of 4-nitrophenol and methylene blue by biogenic gold nanoparticles synthesized using *Carpobrotus edulis* fruit (sour fig) extract

Nanomaterials and Nanotechnology
Volume 12: 1–14
© The Author(s) 2022
Article reuse guidelines:
sagepub.com/journals-permissions
DOI: 10.1177/18479804221108254
journals.sagepub.com/home/nax


Abram M Madiehe^{1,2} , Koena L Moabelo^{1,2} , Keletso Modise^{1,2} , Nicole RS Sibuyi² , Samantha Meyer³, Admire Dube⁴ , Martin O Onani⁵  and Mervin Meyer² 

Abstract

Along with the increasing requirement for efficient organic conversions using green chemistry, there is a need to develop highly efficient and eco-friendly catalytic reaction systems. Gold nanoparticles (AuNPs)-based nanocatalysts are promising candidates for the reduction of environmental pollutants, such as nitroaromatics and dyes. This study reports on the green synthesis of AuNPs using *Carpobrotus edulis* (*C. edulis*) fruit aqueous extract (CeFE) and their catalytic activities. The CeFE induced rapid reduction of gold (III) salt to form monodispersed and spherical AuNPs, with a core and hydrodynamic sizes of 40 and 108.7 nm, respectively. CeFE alone had no effect on 4-nitrophenol, whereas incubation with methylene blue (MB) caused reduction of the peak at 665 nm. Addition of CeFE-AuNPs in the presence of NaBH₄, caused the reduction of 4-nitrophenol to 4-AP, and MB to leucoMB within 10 min. These reactions followed the pseudo first-order kinetics. Therefore, biogenic CeFE-AuNPs could be used for the elimination of noxious environmental pollutants.

Keywords

Gold nanoparticles, catalytic activity, 4-nitrophenol, methylene blue, plant polyphenols, green synthesis

Topic Area: Nanoparticles and Colloids
Topic Editor: Leander Tapfer
Associate Editor: Leander Tapfer

Introduction

The high impact of nanotechnology on many important areas such as medicine, energy, electronics, transport and space has created a surge in creating greener systems and approaches to solve major health, environmental and energy challenges. Nanotechnology is mainly geared towards the manufacturing of materials that are 10⁻⁹ m in size,¹ where at this size they possess unique physical and chemical properties with novel applications.² The application of green chemistry principles in nanotechnology for the synthesis of biogenic nanomaterials can help resolve the limitations

¹Nanobiotechnology Research Group, Department of Biotechnology, University of Western Cape, Bellville, South Africa

²DSI/Mintek Nanotechnology Innovation Centre, Biolabels Node, Department of Biotechnology, University of Western Cape, Bellville, South Africa

³Department of Biomedical Sciences, Faculty of Health and Wellness Sciences, Cape Peninsula University of Technology, Bellville, South Africa

⁴Nanomedicine Research Group, School of Pharmacy, University of Western Cape, Bellville, South Africa

⁵Chemistry Department, University of Western Cape, Bellville, South Africa

Corresponding author:

Abram M Madiehe, Nanobiotechnology Research Group, Department of Biotechnology, University of Western Cape, Private Bag x17, Bellville 7535, South Africa.

Email: amadiehe@uwc.ac.za



Creative Commons CC BY: This article is distributed under the terms of the Creative Commons Attribution 4.0 License (<https://creativecommons.org/licenses/by/4.0/>) which permits any use, reproduction and distribution of the work without further permission provided the original work is attributed as specified on the SAGE and Open Access pages (<https://us.sagepub.com/en-us/nam/open-access-at-sage>).

associated with the conventional methods of synthesis i.e. the chemical and physical approaches. Green synthesis has potential to reduce the use and generation of hazardous substances during the manufacturing and application of nanoparticles (NPs) produced through the conventional methods.^{3,4} Biogenic NPs are considered to be more safe, eco-friendly, biocompatible and less toxic when compared to the chemically synthesized NPs.⁵

Green synthesis of NPs can be accomplished using plant extracts (also called phytosynthesis) and microorganisms. Plant extract-based synthesis has distinctive features such as a higher rate of NPs formation compared to the synthesis rate using microorganisms, no additional reagents are required for synthesis, and the NPs are easy to clean-up, and up-scale.⁶⁻⁸ In addition, plant extracts contain a wide range of biomolecules and metabolites, such as terpenoids, vitamins, polysaccharides, proteins, alkaloids, phenolic compounds, enzymes, etc.,⁸ which can act as reducing and capping/stabilizing agents in the synthesis of NPs.⁹⁻¹² Plant extracts-based NPs have a large range of biological properties, such as antibacterial, antifungal, anticancer, anti-biofouling, anti-malarial, anti-parasitic, antioxidant^{6,13,14} and catalytic activity.¹⁴⁻¹⁷

The use of green-synthesized AuNPs in catalysis, especially for their catalytic reduction of the environmental pollutants, such as p-nitrophenols, are well studied.¹⁴⁻¹⁷ These pollutants are by-products in the production of herbicides, pesticides and synthetic dyes, and the US Environmental Protection Agency (EPA) has classified them as priority pollutants due to their toxicity. Green synthesized biogenic AuNPs have successfully reduced these pollutants to p-aminophenols in the presence of sodium borohydride (NaBH_4).^{16,18,19} Due to the high surface area, AuNPs and other NPs show greater catalytic activity at lower concentrations compared to traditional catalysts.^{20,21} As catalysts, AuNPs are also easy to recover, can be reused several times, and the final product is metal free.²⁰ In contrast, the conventional environmental remediation approaches for the degradation of nitroaromatic compounds are harmful to the environment.^{22,23}

In this study, *C. edulis*, a South African ground cover succulent plant belonging to the family *Aizoaceae*,²⁴ was used for the synthesis of AuNPs. It originated along the coastline of Namaqualand in the Northern Cape, and south and eastwards along the coastline of the Western and the Eastern Cape Provinces.²⁴ From there, members of this family have been introduced as ornamental plants in gardens, parks and on roadsides and for erosion control in many sub-tropical and temperate countries such as Europe, USA, Australia, New Zealand, South America, North Africa, and Pacific and Atlantic Islands. This superb water-wise plant has recognized traditional medicinal properties, such as antimicrobial,²⁵⁻²⁷ antioxidant^{25,28-30} and antiviral²⁴ properties. The leaf pulp and juice of *C. edulis*

contain hydrolysable tannins that have a diverse range of pharmacological properties.³¹⁻³³ *C. edulis* bears large yellow flowers that develop into conical, fleshy fruit capsules, which turn reddish-brown when ripe, called sour figs (Figure 1).

The fruit contains an edible sweet-sour slimy pulp with slimy brown seeds and has a strong, astringent taste. The common medicinal use of sour figs is for purgation,³³ while the dried fruits are processed into jam or added to curry dishes. However, huge amounts of this fruit end up as waste in landfills or are discarded with the dried plants. Therefore, we explored the potential industrial applications for this fruit. So far, and to the best of our knowledge, there is no report on the green synthesis of AuNPs using the *C. edulis* fruit extract. Therefore, the current study reports on the synthesis of CeFE-AuNPs and an investigation of their catalytic activity against 4-nitrophenol and MB.

Materials and Methods

Preparation of CeFE

Dried *C. edulis* fruits (sour figs) were purchased from the local fruit and vegetable market (Bellville Market, South Africa). One hundred grams of dried *C. edulis* fruits were cleaned and washed with distilled water. The washed fruits were steeped in 400 ml of deionized water overnight and cut into halves using a sterile surgical blade. The soft fruits were homogenized using a blender. The homogenate was heated to 80°C for 10 min, and thereafter cooled to ambient room temperature. The cooled homogenate was filtered, first using glass wool, followed by Whatman No. 1 filter paper. The volume of the filtrate was adjusted to 400 ml, in order to obtain 0.25 g/ml extract concentration. The pH of the extract was adjusted from pH of 3 to pH 4 up to 10 by addition of 1 M NaOH.

HPLC analysis of the polyphenols

Phenolic compounds present in CeFE were identified using HPLC following a previously published protocol.³⁴⁻³⁶ The extract was filtered through a 0.22 μm PTFE filter membrane. The solvents used were water (A) and methanol (B), acidified with 0.1 % formic acid and served as mobile phase at a rate of 0.2 ml/min. Gradient elution was applied as isocratic 5% B from 0 – 3 min, a linear gradient increasing from 5 % - 100 % B from 3 – 43 min, kept at 100 % B from 43 – 61 min, a linear decreasing gradient from 100 % to 5 % B from 62 – 70 min. The temperature was kept at 25°C. The column was combined with a Q-exactive orbitrap mass spectrometer, and the spectra was recorded in positive and negative ion mode, respectively.



Figure 1. Photographs of *C. edulis* flower (a), fruit capsules (b) and dried sour figs (c).

Synthesis and optimization of biogenic CeFE-AuNPs

CeFE-AuNPs were synthesized by heating $\text{NaAuCl}_4 \cdot x\text{H}_2\text{O}$ to a desired temperature for 5 min, and subsequent addition of CeFE in a 9:1 ratio. The formation of the CeFE-AuNPs was confirmed by change in colour from light yellow to ruby-red. Various parameters were tested to obtain the optimum conditions: temperature (25, 37, 50, 80 and 99°C), pH of extract (2.9 – 10), concentrations of gold (0.1, 0.25, 0.5 and 1 mM) and CeFE (0.25, 0.5 and 1 g/ml). The reaction was continued for 1 h while shaking in the orbital shaker at 1000 rpm (Eppendorf Thermomixer Comfort, Hamburg, Germany), then cooled to ambient room temperature. The tubes were centrifuged at 14,000 rpm for 15 min at room temperature. The pellets were washed 3 times with deionised water before characterization.

CeFE-AuNPs Characterization

UV-Vis Spectroscopy. UV-Vis spectrophotometer was used to confirm the formation of AuNPs. Exactly 0.03 ml of the CeFE-AuNPs samples were mixed with 0.27 ml of de-ionized water in a 96-well flat-bottom microplate. The absorbance was read in the wavelength range of 300 - 700 nm using the POLARstar Omega microplate reader (BMG Labtech, Offenburg, Germany).

Size and Hydrodynamic Density. CeFE-AuNPs sample was diluted 10-times to 1 ml. The particle size distribution, polydispersity index (PDI) and zeta potential measurements of the CeFE-AuNPs were analysed using a Malvern NanoZS90 Zetasizer (Malvern Instruments Ltd., Malvern, UK) at a scattering angle of 90° at 25°C. The data was analyzed with Zetasizer software version 7.11.

HRTEM. One drop of the CeFE-AuNPs solution was loaded onto a carbon coated copper grid. The grids were dried for a few minutes under a Xenon lamp. The High Resolution TEM (HRTEM) images were captured using FEI Tecnai G² 20 field-emission gun (FEG) HRTEM operated in bright field mode at an accelerating voltage of 200 kV. The elemental composition of the AuNPs was characterized using

EDX liquid nitrogen-cooled lithium-doped Silicon detector. These analyses were performed by the Electron Microscopy Unit, UWC Department of Physics.

FTIR Spectroscopy. The FTIR analysis was performed using the PerkinElmer Spectrum One FTIR spectrophotometer (Waltham, MA, USA) according to the previously reported method.¹³ The dried CeFE and CeFE-AuNPs were mixed with the KBr powder and pressed into a round disk. A pure KBr disk was used for background correction.

Total phenolic content analysis. The total phenolic content (TPC) of CeFE was determined using Folin-Ciocalteu reagent (Sigma-Aldrich, USA) as described previously.³⁷ Total polyphenols were expressed as milligrams Gallic Acid Equivalents per ml of extract (mg GAE/ml).

Catalytic Reduction of 4-Nitrophenol and MB

The reduction of 4-nitrophenol and MB was carried out at room temperature in a 96-well flat-bottom plate as previously described.^{16,22,38-40} The reaction mixture consisted of 0.14 ml water, and 0.03 ml of 2 mM 4-nitrophenol or MB, 0.1 ml 0.03 M sodium borohydride and 0.03 ml CeFE-AuNPs. The absorption spectra were read in the 200 - 750 nm wavelength range using the POLARstar Omega microplate reader at 1 min intervals from 1 to 10 min, thereafter at 5 min intervals to 60 min.

Determination of 4-nitrophenol reduction to 4-AP by HPLC

The conversion from 4-nitrophenol to 4-AP was determined using reverse phase high performance liquid chromatography (RP-HPLC), as previously described.¹⁶

Results

Characterization of CeFE

The preparation of CeFE was carried out as described above. The average pH of the CeFE filtrate was $\sim 2.9 \pm$

Table 1. Identification of CeFE polyphenols by HPLC analysis.

| Polyphenols | Type | Sample Conc. (mg/g) |
|--------------|---------------|---------------------|
| Epicatechin | Flavanol | 0.967 ± 0.062 |
| EGCG | Flavanol | 0.345 ± 0.083 |
| Catechin | Flavanol | 1.265 ± 0.051 |
| Ferulic acid | Phenolic acid | 0.022 ± 0.004 |
| Myricetin | Flavanol | 0.043 ± 0.003 |
| Rutin | Flavanol | 0.417 ± 0.073 |

0.56. Increasing the pH of the extract from 3 to 10, was associated with colour change from a yellow to a deep brownish colour at pH 10. The increase in pH was further associated with precipitation of unidentified macromolecules, which were removed by centrifugation. The TPC and the polyphenols in CeFE were determined following the removal of the precipitate by spectrophotometry and HPLC, respectively. The TPC content was determined to be 131.6 ± 1.16 mg/g. HPLC analysis revealed the presence of some of the main polyphenolic compounds in the CeFE, as indicated in Table 1. Catechin, epicatechin, rutin, myricetin and epigallocatechin gallate (EGCG) were the most abundant flavonols in the extract. However, ferulic acid was the only phenolic compound identified in the CeFE, using available standard compounds. Various compounds have been identified using an extensive HPLC-ESI-LC-MS/MS,^{30,34,41} and corroborated our findings of the five compounds.

CeFE-AuNPs synthesis and characterization

CeFE-AuNPs were synthesized with CeFE at different pH conditions (2.5 – 10) by varying one factor at a time, namely: temperature, gold salt and CeFE concentrations. These four parameters are known to strongly affect the hydrodynamic size and shapes of NPs.^{42,43} The formation of CeFE-AuNPs was confirmed by both changes in colour from light yellow to a ruby-red colour and UV-Vis spectroscopy.

UV-Vis characterization. Temperature and pH have been shown to have great impact on the synthesis of AuNPs.⁴⁴ As shown in Figure 2, the reduction of gold ions into AuNPs by CeFE was evidenced by the UV-Vis spectra showing characteristic, well-defined surface plasmon resonance (SPR) band at around 535 - 540 nm.

This phenomenon is attributed to the excitation of the SPR of AuNPs. All pH and temperatures tested produced AuNPs. The pH ranging from 2.5 to 8 produced CeFE-AuNPs that were approximately 100 nm in size, as determined by dynamic light scattering (DLS). CeFE at pH 9 and 10 produced redshifted AuNPs, which suggested that larger

AuNPs were produced or that aggregation had occurred. DLS analysis of pH 9 and 10 samples revealed that the synthesized AuNPs had a small size range (23.57 – 60.77 nm) and higher PDI range (0.805 – 0.350), thus indicating polydispersity. Coupled with the blue colour of the AuNPs at basic pH, the NPs were considered unstable. This instability could be due to insufficient amounts of CeFE phytochemicals to cap the AuNPs.

These results confirmed the vital role played by pH in controlling the shape and size of the AuNPs. It has been shown that protonation and deprotonation surface reactions are used to obtain local surface charge which depends on particle size and pH.⁴⁵ At higher pH, the large number of phenolic functional groups available for gold binding possibly facilitated a higher number of Au⁺ ions to rapidly nucleate and subsequently form a large number of AuNPs with smaller diameters. It was observed that, if the unknown pH-precipitated material is not removed by centrifugation, this tended to inhibit the formation of AuNPs. Therefore, the impact of the removal of these unknown materials, which could possibly include proteins, amino acids and other phytochemicals that are pH sensitive, in the synthesis of AuNPs is currently unknown and will be further investigated.

Temperature effects were also explored for the synthesis of CeFE-AuNPs (Figure 2). Lower temperatures (25 – 50°C) favoured the formation of CeFE-AuNPs with higher yields (Figure 3(a)) which is represented by the peak intensities and the Amax (Figure 3(b)), the higher the absorbance of the AuNPs the higher the concentration of the AuNPs formed. These AuNPs had a larger hydrodynamic sizes and uniform size distribution (Figure 3(c)), which is in accordance with previous reports.^{44,46,47} Since the CeFE-AuNPs produced at lower temperatures had similar properties, 25°C was selected as an optimal temperature to fabricate the CeFE-AuNPs. This bodes well for the green chemistry principles, as no external energy was required for the synthesis of CeFE-AuNPs. The optimum pH was pH 8 (Figure 3), because the UV-Vis spectrum was narrow and symmetrical. This suggested that the CeFE-AuNPs were monodispersed.

Moreover, increasing temperature was associated with reduced synthesis (yield) of CeFE-AuNPs at pH 8 (Figures

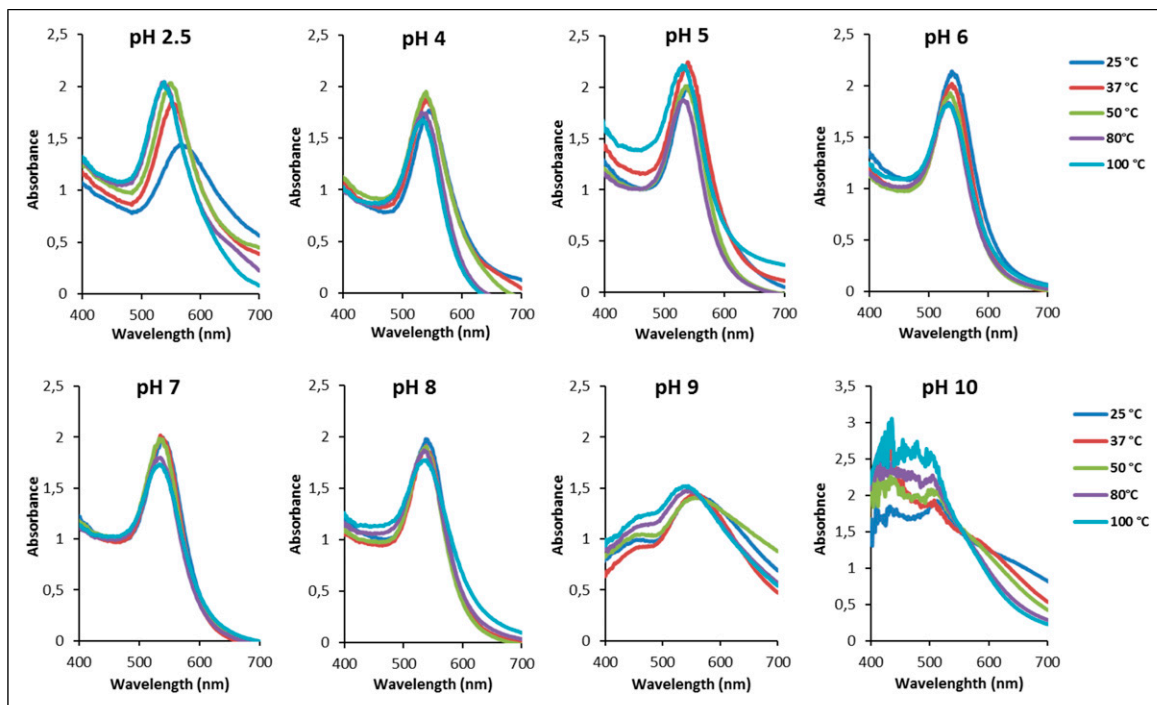


Figure 2. UV-Vis spectra for the synthesis of CeFE-AuNPs at different pH and temperature conditions.

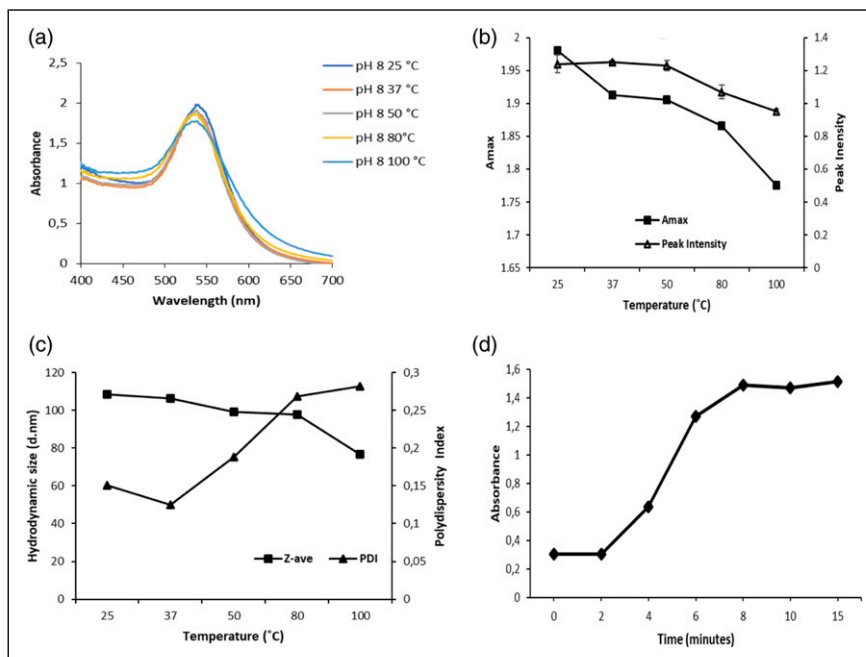


Figure 3. The effects of temperature on the synthesis of CeFE-AuNPs using CeFE at pH 8. a) UV-Vis spectra at different temperatures; b) effect of temperature on the yield (maximum absorbance/Amax and peak intensity) of CeFE-AuNPs; c) effect of temperature on size and PDI, and d) the rate of synthesis of CeFE-AuNPs.

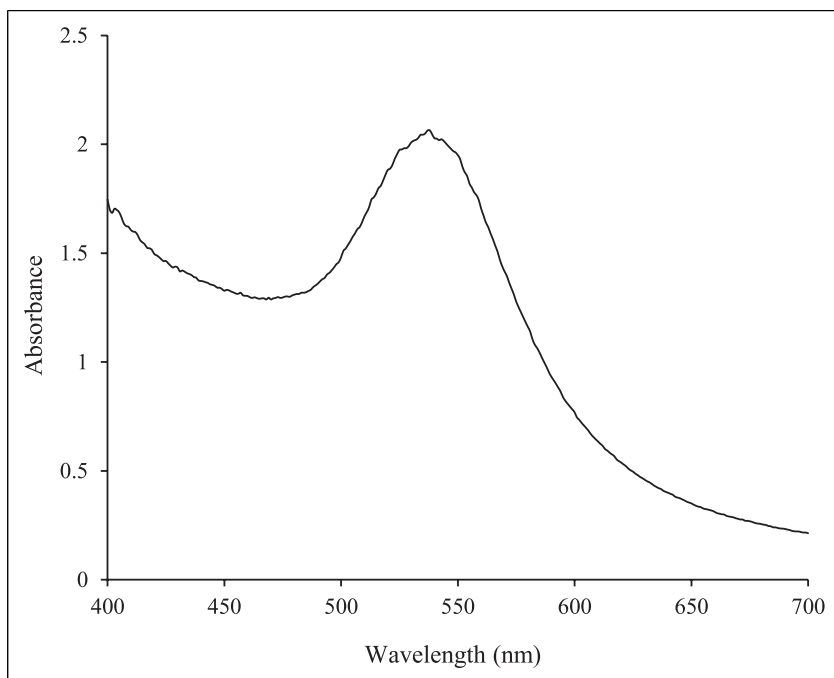


Figure 4. UV-Vis spectrum of CeFE-AuNPs synthesized at the optimal conditions. The CeFE-AuNPs were synthesized at 25°C with pH 8 CeFE (0.25 g/ml) and 0.5 mM gold salt.

3(a) and (b)), and this was further associated with increases in polydispersity and reduction in the hydrodynamic size of AuNPs (Figure 3(c)). The synthesis of CeFE-AuNPs reached saturation within a minimum time of 8 min, and the synthesis was completed after 15 min (Figure 3(d)).

The results further confirm that temperature is also an important parameter for the synthesis of CeFE-AuNPs. Previous studies have shown that lower temperatures favour the formation of larger AuNPs, and higher temperatures favour the formation of smaller AuNPs.^{44,48,49} This is attributed to the fact that increasing the reaction temperature led to a rapid reduction of the metal precursors, and the subsequent homogeneous nucleation of gold nuclei, allowing for the formation of smaller spherical AuNPs. Furthermore, it has been well demonstrated that the synthesis of AuNPs using certain plant extracts require heat activation, but only to a certain point.^{50,51} This is because certain reducing agents in the plant extract gets inactivated at higher temperatures. This phenomenon is also seen by the decrease in absorbance at 100°C and the increase in absorbance or peak intensity at 25 – 50°C.

The concentrations of CeFE and gold solution required for CeFE-AuNPs synthesis were optimized as shown in Supplement Figure S1. The NaAuCl₄·xH₂O concentration at 0.1 and 1 mM was either insufficient or too high to synthesize stable AuNPs at 25°C for all CeFE concentrations, respectively. CeFE-AuNPs with desired optical properties were synthesized at 0.25 and 0.5 mM of

NaAuCl₄·xH₂O at 0.125 – 0.5 g/ml of CeFE. The optimal conditions were thus selected as 0.25 g/ml of CeFE at pH 8 and 0.5 mM NaAuCl₄·xH₂O, because the UV-Vis spectrum was narrower, and the SPR was higher than that of the 0.5 mM NaAuCl₄·xH₂O and 1 g/ml CeFE. The synthesis was scaled-up using these optimized conditions, and the UV-Vis of the CeFE-AuNPs is shown in Figure 4, with an SPR peak at 535 nm, A_{max} of 2.1 and a peak intensity of 1.3.

Furthermore, the analysis of the absorption maxima for CeFE-AuNPs at various pH conditions explicitly depicted a gradual shift towards lower wavelengths with an increasing pH from 3 to 7, indicating that the sizes of the particles decreased when pH changed from highly acidic to neutral i.e., from 3 to 7. When the pH was increased from 7 to 10, the absorption maxima shifted towards higher wavelengths, which suggested that the size of the NPs increased when pH is increased from 7 to 9. Taken together, this suggested that the synthesis of smaller CeFE-AuNPs can be synthesized when the pH of the CeFE is around 7. This data is corroborated by Singh & Srivastava.⁵²

DLS and TEM characterization. DLS and TEM were used to determine the size, shape and morphologies of CeFE-AuNPs synthesised from CeFE produced at pH 8. The DLS showed size distribution in the range of 50 to 200 nm, with an average hydrodynamic size of 108.0 ± 0.2 nm (Figure 5(a)). It is possible that the NPs were synthesized

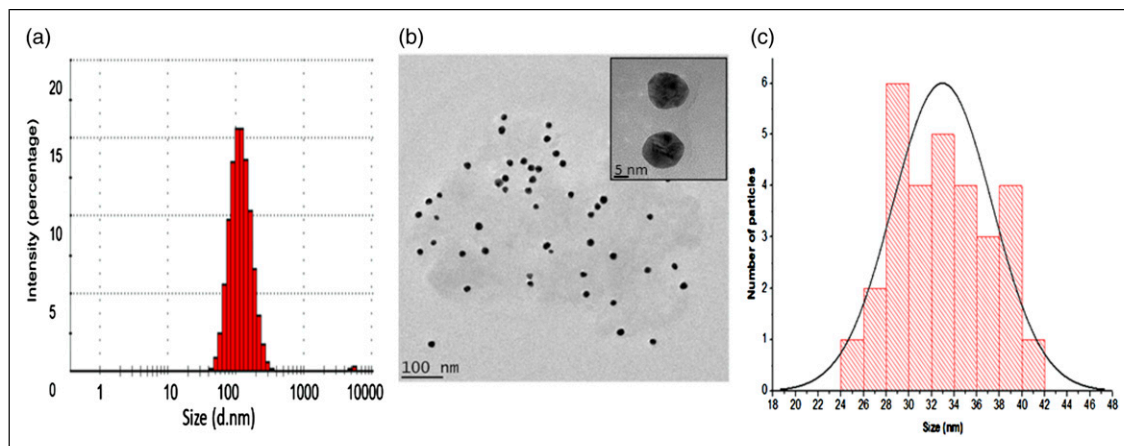


Figure 5 Size distribution of CeFE-AuNPs as measured by DLS (a) and TEM (b). The core size distribution from the TEM micrograph was analysed by ImageJ with Gaussian fitting and represented as a histogram (c).

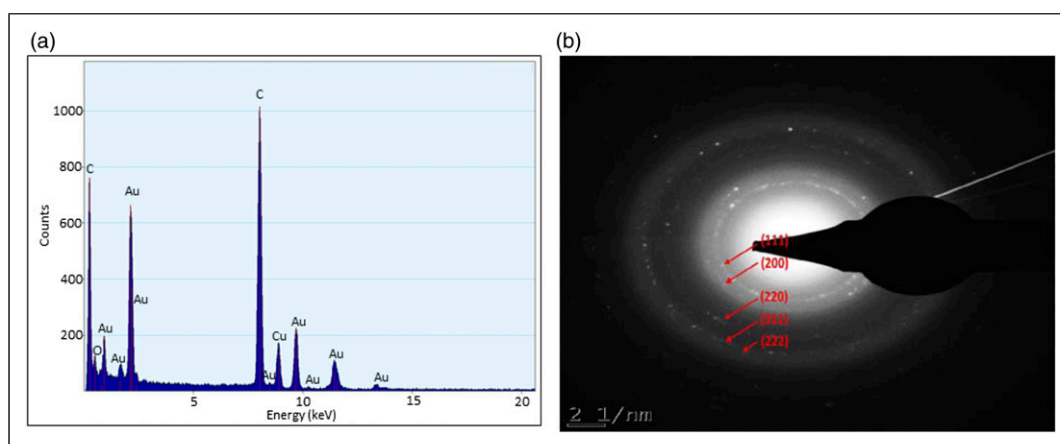


Figure 6. The EDX spectrum (a) and SAED pattern (b) of the synthesized CeFE-AuNPs. These are representative images of 3 independent experiments done in triplicate.

from a combination of different phytochemicals. The TEM images indicated that the CeFE-AuNPs obtained were mostly spherical in shape, with an average core size of 32.96 ± 4.39 nm (Figures 5(b) and (c)). Furthermore, the AuNPs had a “halo” (Figure 5(b): insert), which is indicative of an organic capping layer around the NPs surface.⁵³

The mean particle size determined by the TEM analysis was significantly smaller (33 nm) than that measured by the DLS (108 nm). The adsorption of organic stabilizers from the extract on the surface of AuNPs, and the adsorption of water on the stabilized AuNPs could be responsible for this discrepancy, which could have had an effect on the average particle hydrodynamic size obtained by the DLS.^{54–56} Therefore, CeFE served as a good reducing and a capping agent in the synthesis of AuNPs and yielded mono-dispersed AuNPs. Since these analyses were performed for the optimized CeFE-AuNPs samples, it is unknown whether

AuNPs synthesised at other pH values would give the same results, as different green synthesis methods have been shown to synthesize quasi-spherical AuNPs with an average diameter ranging between 40 and 100 nm.¹³

EDX spectrum and SAED pattern. The EDX spectrum showed strong signals for gold atoms, with the strongest signal peak at 2.3 keV,⁵⁷ demonstrating that the AuNPs have been formed (Figure 6(a)). The elements such as C, O and Cu were also detected. The C and O could be from the organic compounds present in the extract that played a role in the reduction and stability of the AuNPs. The Cu in the spectrum was from the carbon-coated copper grid used for TEM analysis. As shown in Figure 6(b), SAED pattern analysis indicated the Miller indices at (111), (200), (220), (311), and (222), indicating that the synthesized AuNPs have a phase crystal of face-centred cubic.⁵⁸ The formation

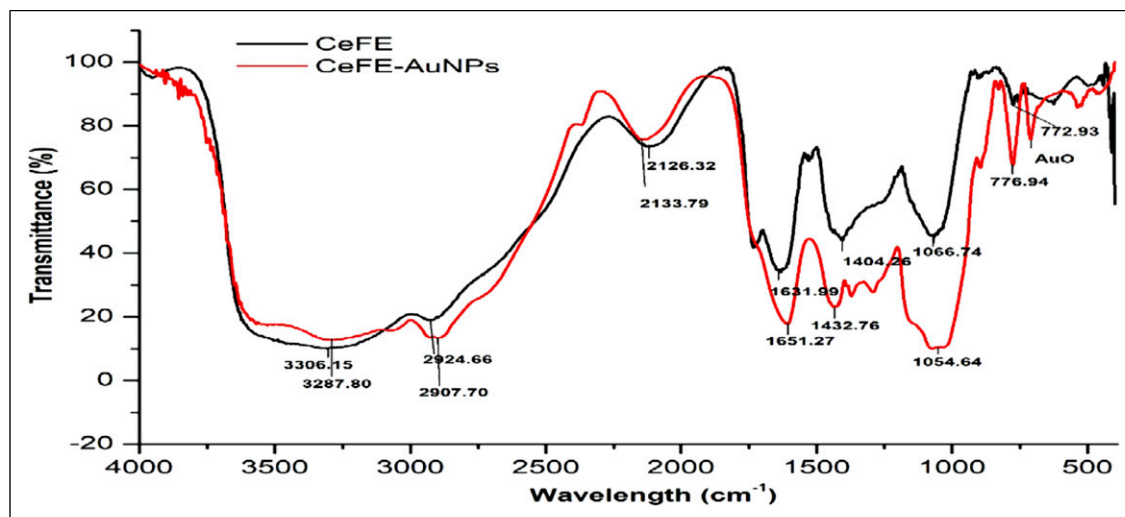


Figure 7. FTIR analysis of the CeFE and the CeFE-AuNPs.

Table 2. Shifts of the FTIR spectra bands (cm^{-1}) of major peaks of CeFE and CeFE-AuNPs.

| CeFE | CeFE-AuNPs | Shift values | Functional groups |
|---------|------------|--------------|--|
| 3306.15 | 3287.80 | +18.35 | OH, NH |
| 2924.66 | 2907.57 | +17.09 | CH |
| 2126.32 | 2133.79 | - 7.47 | $\text{C}\equiv\text{C}$ |
| 1631.99 | 1615.27 | +16.72 | NH, $\text{C}=\text{O}$, $\text{C}=\text{N}$ |
| 1404.26 | 1432.76 | - 28.5 | $\text{C}=\text{O}$, CH, OH |
| 1066.74 | 1054.64 | +12.1 | $\text{C}-\text{O}/\text{NH}$, $\text{C}-\text{O}-\text{C}/\text{CN}$ |
| 772.93 | 776.94 | - 4.01 | CH |

Note: The shift values were calculated by subtracting the peak transmittance of the AuNPs from that of the extract.

of AuNPs and their crystal phase was in accordance with the Joint Committee on Powder Diffraction Standards of Au (JCPDS number 04-0784).⁵⁸

FTIR analysis. The FTIR spectroscopy revealed the surface chemistry of the CeFE-AuNPs compared to CeFE (Figure 7). The band at 3306.15 cm^{-1} is assigned to the O–H and N–H stretching vibration of carboxylic acid and proteins from the extract. The peak at 1631.99 cm^{-1} corresponds to the bending vibration of amide I, and this arises due to the carbonyl stretching vibration in the amide linkage of proteins.⁵⁹

Such observations suggest the presence and binding of proteins with AuNPs, which may be involved in the process of their formation and stabilization. The bonds that are assumed to be involved in the formation of CeFE-AuNPs are shown in Table 2.

The spectrum of the CeFE-AuNPs exhibited absorption bands at 3287.8 , 2907.6 , 1615.3 , 1432.8 , 1054.6 and 776.9 cm^{-1} . These bands are associated with

polyphenols.²² Comparison of the free CeFE and CeFE-AuNPs polyphenols indicated shifts in the absorption bands of the carbonyl, hydroxyl and aromatic ring groups (Table 2), which further confirmed that the polyphenols are present on the surface of CeFE-AuNPs. Since CeFE has high levels of catechin, epicatechin and EGCG (Table 1) and reducing sugars, these could play a major role in the AuNPs synthesis, as catechin^{60,61} and EGCG⁶² have been shown to produce AuNPs with diverse shapes. The possible mechanism of formation of CeFE-AuNPs is shown in Figure 8.

Catalysis

Reduction of 4-nitrophenol. The catalytic activity of green synthesized AuNPs using various plant extracts have been reported.^{38,63–69} CeFE-AuNPs also displayed catalytic activity in the reduction of 4-nitrophenol to 4-AP (Figures 9(a) and (b)) and MB to leucoMB (Figures 9(c) and (d)) by NaBH_4 . In this study, CeFE-AuNPs act as a catalyst and overcome the kinetic barrier of hydrogenation and facilitate the electron exchange between the donor and acceptor (Figure 9). Addition of NaBH_4 to a light yellow 4-nitrophenol solution resulted in the formation of a bright green solution, which showed an absorption peak at 400 nm, due to the formation of the 4-nitrophenolate anion. The CeFE did not show any catalytic activity when added to the 4-nitrophenol and NaBH_4 solution (Supplemental Figure S2), only the 4-nitrophenol conversion to 4-nitrophenolate anions occurred but there was no formation of 4AP up to 60 min. In contrast, addition of CeFE-AuNPs resulted in the reduction of 4-nitrophenol to 4-nitrophenolate anion, with the concomitant appearance of a peak at 300 nm because of the 4-AP formation (Figure 9(a)). This reaction was very rapid and completed within 10 min when using as-synthesized CeFE-AuNPs, with a reaction rate of $3.3 \times 10^{-3}\text{ s}^{-1}$ (Figure 9(b)). This rate is equivalent to the

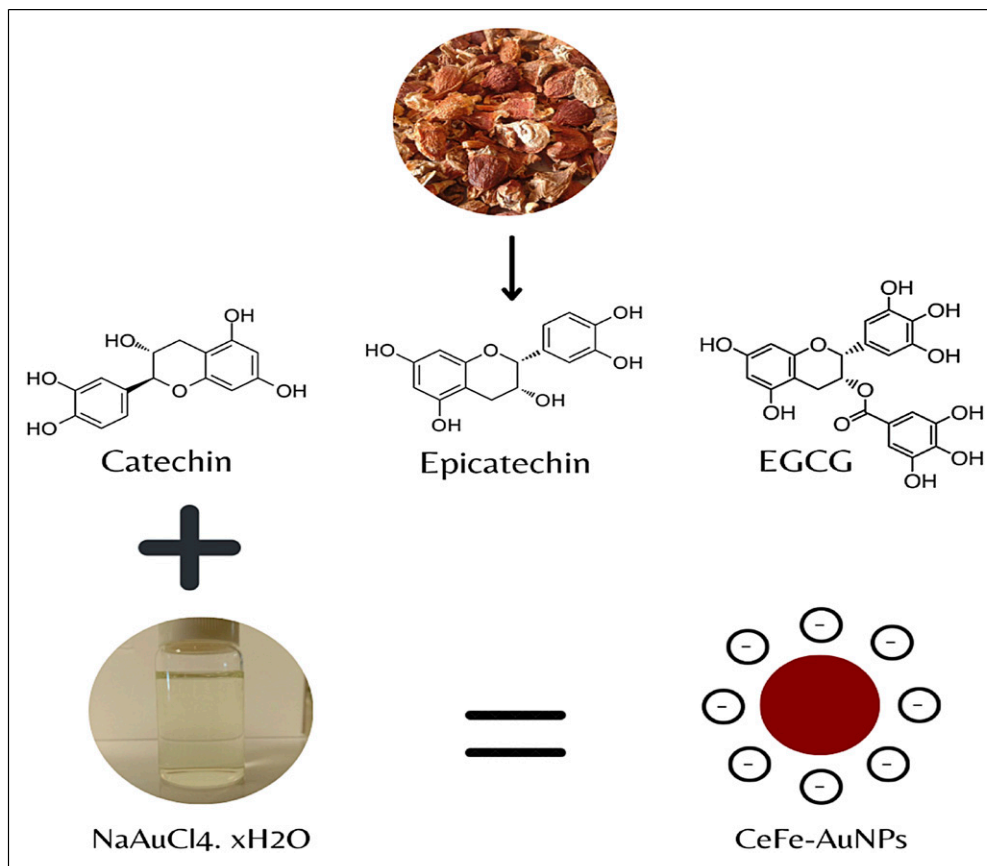


Figure 8. Green synthesis of AuNPs by CeFE. Chemical structures of abundant compounds in CeFE, which may be responsible for the reduction of Au^+ ions and synthesis of CeFE-AuNPs.

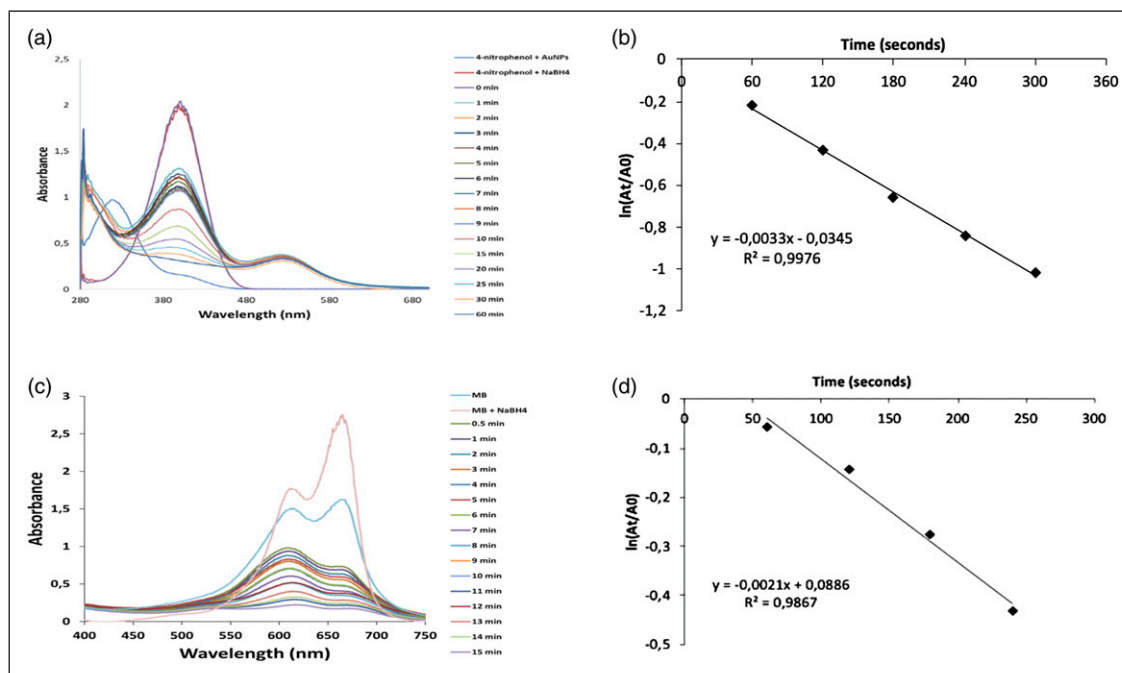


Figure 9 UV-Vis spectra showing the catalytic reduction of 4-nitrophenol (a) and MB (c) by NaBH_4 in the presence of CeFE-AuNPs. Plots of the pseudo-first order reaction kinetics for the reduction of 4-nitrophenol (b) and MB (d) by CeFE-AuNPs in the presence of NaBH_4 .

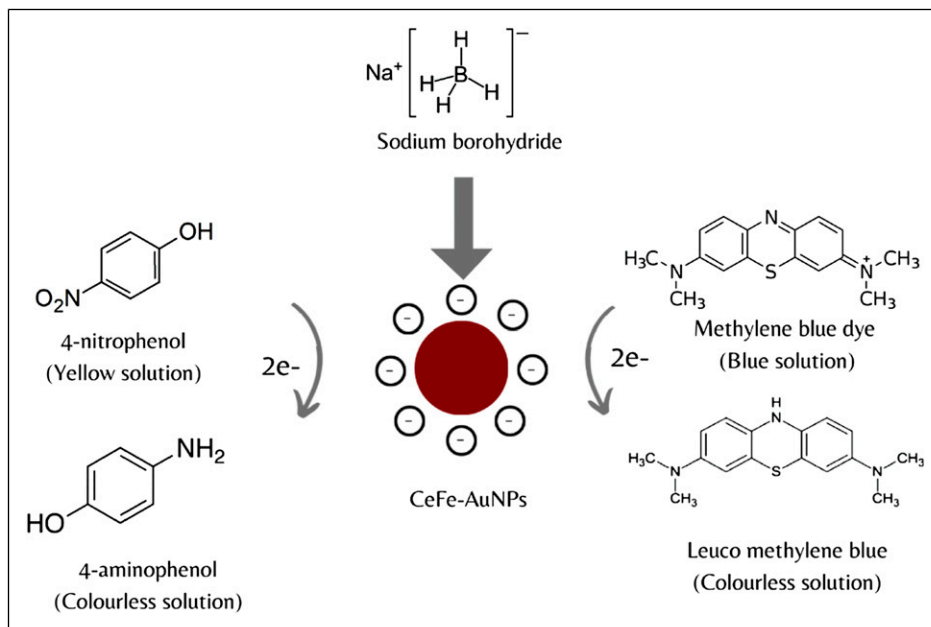


Figure 10. Possible mechanism of catalytic reduction of 4-nitrophenol and MB dye with NaBH₄ in the presence of CeFe-AuNPs.

catalytic activity of caffeic acid-AuNPs.¹⁶ CeFe-AuNPs completely catalysed the reduction of 0.2 mM 4-nitrophenol to 4-AP in the presence of NaBH₄, with no residual 4-nitrophenol, as confirmed by HPLC.

Reduction of MB. Addition of CeFE to a light blue MB solution resulted in the formation of a dark blue solution, which was associated with a decrease in the absorption peak at 665 nm. Addition of CeFe-AuNPs resulted in similar characteristics. However, no further reduction of the peak occurred over time, indicating that, in the absence of NaBH₄, no activity was possible. Addition of NaBH₄ to CeFE+MB resulted in further decrease of the peak at 665 nm. In contrast, addition of CeFe-AuNPs resulted in the reduction of MB to leucoMB over time (Figure 9(c)). This reaction was very rapid and completed within 10 min when using as-synthesized CeFe-AuNPs, with a reaction rate of $1.33 \times 10^{-3} \text{ s}^{-1}$ (Figure 9(d)).

The above reaction kinetics were in good agreement with the pseudo-first order equation: where A_t is the absorbance at different time points, k_{app} is the apparent rate constant, and t is the reaction time (in seconds). These results are consistent with previously published studies on the catalytic capacity of biogenic/green synthesized AuNPs.⁷⁰⁻⁷² The possible mechanism of catalytic action of CeFe-AuNPs is depicted in Figure 10. The role of AuNPs in these reactions is still not clear, however, studies have speculated that the NPs as catalysts might possibly overcome the kinetic barrier of hydrogenation and facilitate electron relay from the donor to the acceptor.⁷³ In this case, the CeFe-AuNPs speed up the degradation of the two dyes by facilitating the electron

exchange between NaBH₄ and 4-nitrophenol, as well as NaBH₄ and MB dye. The reduction of these compounds formed 4-AP and leucoMB, respectively. The catalytic activity and efficiency of AuNPs are dependent on their size, shape, surface composition and pH⁷⁴; and have been reported to have enzyme-like catalytic activities as either antioxidant or pro-oxidant agents.⁷³

Conclusion

A facile one-step green synthesis protocol that utilizes CeFE as a reducing, capping and/or stabilizing agent to generate highly stable CeFe-AuNPs has been developed. This method produced spherical AuNPs that were characterized using various techniques. These biogenic AuNPs possessed high catalytic activity for the reduction of 4-nitrophenol to 4-AP and MB to leucoMB, respectively, and could be useful in the elimination of these environmental pollutants. If not consumed, this fruit would have ended up as waste, but instead was used to produce AuNPs at low cost that can be used to clean up water pollutants. The synthesised AuNPs can also be retrieved and used in another catalytic reaction, further emphasizing their low cost. The eco-friendliness of these AuNPs will be evaluated in future.

Acknowledgements

The authors acknowledge the Department of Science and Innovation/Mintek Nanotechnology Innovation Centre Biolabels Unit for funding this project. The authors thank the UWC Departments of Physics and Chemistry for their assistance with

HRTEM and FTIR analyses, respectively. The authors thank Dr. Sarah D'Souza for HPLC analysis of 4-nitrophenol and 4-AP and Mr. Fanie Bezuidenhout at Cape Peninsula University of Technology (CPUT) for TPC and HPLC analysis of CeFE. Nicole Sibuyi is now working at the Health Platform Diagnostic Unit (Advanced Materials Division, Mintek, Johannesburg, South Africa).

Declaration of conflicting interests

The author(s) declared no potential conflicts of interest with respect to the research, authorship, and/or publication of this article.

Funding

The author(s) received financial support for the research, authorship, and/or publication of this article from the Department of Science and Innovation/Mintek Nanotechnology Innovation Centre Biolabels Unit and the University of the Western Cape.

ORCID iDs

Abram M Madiehe  <https://orcid.org/0000-0002-3935-467X>

Koena L Moabelo  <https://orcid.org/0000-0002-9114-4530>

Keletso Modise  <https://orcid.org/0000-0002-1336-5960>

Nicole RS Sibuyi  <https://orcid.org/0000-0001-7175-5388>

Admire Dube  <https://orcid.org/0000-0002-5684-6094>

Martin O Onani  <https://orcid.org/0000-0002-4735-3669>

Mervin Meyer  <https://orcid.org/0000-0002-8296-4860>

Supplemental Material

Supplemental material for this article is available online.

References

- Albrecht MA, Evans CW, and Raston CL. Green chemistry and the health implications of nanoparticles. *Green Chemistry* 2006; 8(5): 417–432. DOI: [10.1039/b517131h](https://doi.org/10.1039/b517131h)
- Wozniak A, Malankowska A, Nowaczyk G, et al. Size and shape-dependent cytotoxicity profile of gold nanoparticles for biomedical applications. *J Mater Sci Mater Med* 2017; 28(6): 92. DOI: [10.1007/s10856-017-5902-y](https://doi.org/10.1007/s10856-017-5902-y)
- Kratosova G, Holisova V, Konvickova Z, et al. From biotechnology principles to functional and low-cost metallic bionanocatalysts. *Biotechnology Advances* 2019; 37(1): 154–176. DOI: [10.1016/j.biotechadv.2018.11.012](https://doi.org/10.1016/j.biotechadv.2018.11.012)
- Sibuyi NRS, Thipe VC, Panjtan-Amiri K, et al. Green synthesis of gold nanoparticles using Acai berry and Elderberry extracts and investigation of their effect on prostate and pancreatic cancer cells. *Nanobiomedicine (Rij)* 2021; 8: 184954352199531. DOI: [10.1177/1849543521995310](https://doi.org/10.1177/1849543521995310)
- Shedbalkar U, Singh R, Wadhvani S, et al. Microbial synthesis of gold nanoparticles: current status and future prospects. *Advances Colloid Interface Science* 2014; 209: 40–48. Retrieved from https://ac.els-cdn.com/S0001868613001929/1-s2.0-S0001868613001929-main.pdf?_tid=ae452936-f00e-471e-ab58-1cfde2095041&acdnt=1530461917_04f71f2cbb01b0a30af258cf42cc0f74
- Noruzi M. Biosynthesis of gold nanoparticles using plant extracts. *Bioprocess Biosyst Eng* 2015; 38(1): 1–14. DOI: [10.1007/s00449-014-1251-0](https://doi.org/10.1007/s00449-014-1251-0)
- Rama P, Baldelli A, Vignesh A, et al. Antimicrobial, antioxidant, and angiogenic bioactive silver nanoparticles produced using *Murraya paniculata* (L.) jack leaves. *Nanomaterials Nanotechnology* 2022; 12: 18479804211056167.
- Stozhko NY, Bukharinova MA, Khamzina EI, et al. The effect of the antioxidant activity of plant extracts on the properties of gold nanoparticles. *Nanomaterials (Basel)* 2019; 9(12): 1655. DOI: [10.3390/nano9121655](https://doi.org/10.3390/nano9121655)
- Ahmad T, Bustam MA, Irfan M, et al. Mechanistic investigation of phytochemicals involved in green synthesis of gold nanoparticles using aqueous *Elaeis guineensis* leaves extract: Role of phenolic compounds and flavonoids. *Biotechnol Appl Biochem* 2019; 66(4): 698–708. DOI: [10.1002/bab.1787](https://doi.org/10.1002/bab.1787)
- Alegria ECBA, Ribeiro APC, Mendes M, et al. Effect of phenolic compounds on the synthesis of gold nanoparticles and its catalytic activity in the reduction of nitro compounds. *Nanomaterials* 2018; 8(5): 320. DOI: [10.3390/nano8050320](https://doi.org/10.3390/nano8050320)
- Lim SH and Park Y. Green synthesis, characterization and catalytic activity of gold nanoparticles prepared using rosmarinic acid. *J Nanoscience Nanotechnology* 2018; 18(1): 659–667. DOI: [10.1166/jnn.2018.13982](https://doi.org/10.1166/jnn.2018.13982)
- Mashwani ZU, Khan MA, Khan T, et al. Applications of plant terpenoids in the synthesis of colloidal silver nanoparticles. *Adv Colloid Interface Sci* 2016; 234: 132–141. DOI: [10.1016/j.cis.2016.04.008](https://doi.org/10.1016/j.cis.2016.04.008)
- Elbagory AM, Cupido CN, Meyer M, et al. Large Scale Screening of Southern African Plant Extracts for the Green Synthesis of Gold Nanoparticles Using Microtitre-Plate Method. *Molecules* 2016; 21(11): 1498. DOI: [10.3390/molecules21111498](https://doi.org/10.3390/molecules21111498)
- Khan T, Ullah N, Khan MA, et al. Plant-based gold nanoparticles; a comprehensive review of the decade-long research on synthesis, mechanistic aspects and diverse applications. *Advances Colloid Interface Science* 2019; 272: 102017. DOI: [10.1016/j.cis.2019.102017](https://doi.org/10.1016/j.cis.2019.102017)
- Qin L, Zeng G, Lai C, et al. Synthetic strategies and application of gold-based nanocatalysts for nitroaromatics reduction. *Science Total Environment* 2019; 652: 93–116. DOI: [10.1016/j.scitotenv.2018.10.215](https://doi.org/10.1016/j.scitotenv.2018.10.215)
- Seo YS, Ahn EY, Park J, et al. Catalytic reduction of 4-nitrophenol with gold nanoparticles synthesized by caffeic acid. *Nanoscale Research Letters* 2017; 12: 7. DOI: [10.1186/s11671-016-1776-z](https://doi.org/10.1186/s11671-016-1776-z)
- Yuan CG, Huo C, Yu SX, et al. Biosynthesis of gold nanoparticles using *Capsicum annum* var. *grossum* pulp extract and its catalytic activity. *Physica E-Low-Dimensional Systems Nanostructures* 2017; 85: 19–26. DOI: [10.1016/j.physe.2016.08.010](https://doi.org/10.1016/j.physe.2016.08.010)

18. Lim SH, Ahn EY, and Park Y. Green synthesis and catalytic activity of gold nanoparticles synthesized by artemisia capillaris water extract. *Nanoscale Research Letters* 2016; 11: 474. DOI: [10.1186/s11671-016-1694-0](https://doi.org/10.1186/s11671-016-1694-0)
19. Park Y and Lim SH. Green gold nanoparticles synthesized using Artemisia capillaris extract and their catalytic performance. *Abstracts Papers American Chemical Society* 2017; 253. Retrieved from <Go to ISI>://WOS:000430568506326.
20. Nasrollahzadeh M and Sajadi SM. Preparation of Au nanoparticles by Anthemis xylopoda flowers aqueous extract and their application for alkyne/aldehyde/amine A(3)-type coupling reactions. *Rsc Advances* 2015; 5(57): 46240–46246. DOI: [10.1039/c5ra08927a](https://doi.org/10.1039/c5ra08927a)
21. Panigrahi S, Basu S, Praharaj S, et al. Synthesis and size-selective catalysis by supported gold nanoparticles: Study on heterogeneous and homogeneous catalytic process. *J Physical Chem C* 2007; 111(12): 4596–4605. DOI: [10.1021/jp067554u](https://doi.org/10.1021/jp067554u)
22. Oueslati MH, Ben Tahar L, and Harrath AH. Synthesis of ultra-small gold nanoparticles by polyphenol extracted from Salvia officinalis and efficiency for catalytic reduction of p-nitrophenol and methylene blue. *Green Chemistry Letters Reviews* 2020; 13(1): 18–26. DOI: [10.1080/17518253.2019.1711202](https://doi.org/10.1080/17518253.2019.1711202)
23. Tan BH, Teng TT, and Omar AKM (2000). Removal of dyes and industrial dye wastes by magnesium chloride. *Water Research*, 34(2), 597–601. DOI: [10.1016/S0043-1354\(99\)00151-7](https://doi.org/10.1016/S0043-1354(99)00151-7)
24. Omoruyi BE, Bradley G, and Afolayan AJ. Antioxidant and phytochemical properties of Carpobrotus edulis (L.) bolus leaf used for the management of common infections in HIV/AIDS patients in Eastern Cape Province. *BMC Complement Altern Med* 2012; 12: 215. DOI: [10.1186/1472-6882-12-215](https://doi.org/10.1186/1472-6882-12-215)
25. Meddeb E, Chami M, Ghazouani T, et al. Biochemical and molecular study of carpobrotus edulis bioactive properties and their effects on dugesia sicula (Turbellaria, Tricladida) Regeneration. *Appl Biochem Biotechnol* 2017; 182(3): 1131–1143. DOI: [10.1007/s12010-016-2387-y](https://doi.org/10.1007/s12010-016-2387-y)
26. Springfield EP and Weitz F. The scientific merit of Carpobrotus mellei L. based on antimicrobial activity and chemical profiling. *African J Biotechnology* 2006; 5(13): 1289–1293. Retrieved from <Go to ISI>://WOS:000238977900022.
27. van der Watt E and Pretorius JC (2001). Purification and identification of active antibacterial components in Carpobrotus edulis L. *J Ethnopharmacology*, 76(1), 87–91. doi:Doi [10.1016/S0378-8741\(01\)00197-0](https://doi.org/10.1016/S0378-8741(01)00197-0)
28. Custodio L, Ferreira AC, Pereira H, et al. The marine halophytes Carpobrotus edulis L. and Arthrocnemum macrostachyum L. are potential sources of nutritionally important PUFAs and metabolites with antioxidant, metal chelating and anticholinesterase inhibitory activities. *Botanica Marina* 2012; 55(3): 281–288. DOI: [10.1515/bot-2012-0098](https://doi.org/10.1515/bot-2012-0098)
29. Geraghty DP, Ahuja KDK, Pittaway J, et al. In vitro antioxidant, antiplatelet and anti-inflammatory activity of Carpobrotus rossii (pigface) extract. *J Ethnopharmacology* 2011; 134(1): 97–103. DOI: [10.1016/j.jep.2010.11.060](https://doi.org/10.1016/j.jep.2010.11.060)
30. Hafsa J, Hammi KM, Ben Khedher MR, et al. Inhibition of protein glycation, antioxidant and antiproliferative activities of Carpobrotus edulis extracts. *Biomedicine Pharmacotherapy* 2016; 84: 1496–1503. DOI: [10.1016/j.biopha.2016.11.046](https://doi.org/10.1016/j.biopha.2016.11.046)
31. Martins M, Ordway D, Kristiansen M, et al. Inhibition of the Carpobrotus edulis methanol extract on the growth of phagocytosed multidrug-resistant Mycobacterium tuberculosis and methicillin-resistant Staphylococcus aureus. *Fito-terapia* 2005; 76(1): 96–99. DOI: [10.1016/j.fitote.2004.09.020](https://doi.org/10.1016/j.fitote.2004.09.020)
32. Ordway D, Hohmann J, Viveiros M, et al. Carpobrotus edulis methanol extract inhibits the MDR efflux pumps, enhances killing of phagocytosed S-aureus and promotes immune modulation. *Phytotherapy Research* 2003; 17(5): 512–519. DOI: [10.1002/ptr.1314](https://doi.org/10.1002/ptr.1314)
33. Springfield EP, Amabeoku G, Weitz F, et al. An assessment of two Carpobrotus species extracts as potential antimicrobial agents. *Phytomedicine* 2003; 10(5): 434–439. DOI: [10.1078/0944-7113-00263](https://doi.org/10.1078/0944-7113-00263)
34. Castañeda-Loaiza V, Placines C, Rodrigues MJ, et al. If you cannot beat them, join them: Exploring the fruits of the invasive species Carpobrotus edulis (L.) NE Br as a source of bioactive products. *Industrial Crops Products* 2020; 144: 112005.
35. Chukwuma CI, Matsabisa MG, Rautenbach F, et al. Evaluation of the nutritional composition of Myrothamnus flabellifolius (Welw.) herbal tea and its protective effect against oxidative hepatic cell injury. *J Food Biochem* 2019; 43(11): e13026. DOI: [10.1111/jfbc.13026](https://doi.org/10.1111/jfbc.13026)
36. Lawal AO, Davids LM, and Marnewick JL. Rooibos (Aspalathus linearis) and honeybush (Cyclopia species) modulate the oxidative stress associated injury of diesel exhaust particles in human umbilical vein endothelial cells. *Phytomedicine* 2019; 59: 152898. DOI: [10.1016/j.phymed.2019.152898](https://doi.org/10.1016/j.phymed.2019.152898)
37. Singleton VL, Orthofer R, and Lamuela-Raventos RM. Analysis of total phenols and other oxidation substrates and antioxidants by means of Folin-Ciocalteu reagent. *Oxidants Antioxidants, Pt A* 1999; 299: 152–178. Retrieved from <Go to ISI>://WOS:000079431900014.
38. Gangula A, Podila R, Ramakrishna M, et al. Catalytic reduction of 4-nitrophenol using biogenic gold and silver nanoparticles derived from Breyenia rhamnoides. *Langmuir* 2011; 27(24): 15268–15274. DOI: [10.1021/la2034559](https://doi.org/10.1021/la2034559)
39. Seoudi R and Said DA. Studies on the effect of the capping materials on the spherical gold nanoparticles catalytic activity. *World J Nano Science Engineering* 2011; 1: 51–61. DOI: [10.4236/wjnse.2011.12008](https://doi.org/10.4236/wjnse.2011.12008)
40. Shen WL, Qu YY, Pei XF, et al. Catalytic reduction of 4-nitrophenol using gold nanoparticles biosynthesized by cell-free extracts of Aspergillus sp WL-Au. *J Hazardous*

- Materials* 2017; 321: 299–306. DOI: [10.1016/j.jhazmat.2016.07.051](https://doi.org/10.1016/j.jhazmat.2016.07.051)
41. Rocha M, Rodrigues M, Pereira C, et al. Biochemical profile and in vitro neuroprotective properties of *Carpobrotus edulis* L., a medicinal and edible halophyte native to the coast of South Africa. *South African Journal Botany* 2017; 111: 222–231.
 42. Hammami I and Alabdallah N. Gold nanoparticles: synthesis properties and applications. *Journal of King Saud University-Science* 2021; 33: 101560.
 43. Patra JK and Baek K-H. Green nanobiotechnology: factors affecting synthesis and characterization techniques. *J Nanomaterials* 2014; 2014: 1–12.
 44. Latif MS, Kormin F, Mustafa MK, et al. Effect of Temperature on the Synthesis of *Centella asiatica* Flavonoids Extract-Mediated Gold Nanoparticles: UV-Visible Spectra Analyses. *AIP Conference Proceedings 2016* 2018; 2016: 020071. DOI: [10.1063/1.5055473](https://doi.org/10.1063/1.5055473)
 45. Barisik M, Atalay S, Beskok A, et al. Size Dependent Surface Charge Properties of Silica Nanoparticles. *J Physical Chem C* 2014; 118(4): 1836–1842. DOI: [10.1021/jp410536n](https://doi.org/10.1021/jp410536n)
 46. Annur S, Santosa SJ, and Aprilita NH. pH Dependence of Size Control in Gold Nanoparticles Synthesized at Room Temperature. *Oriental J Chemistry* 2018; 34(5): 2305–2312. DOI: [10.13005/ojc/340510](https://doi.org/10.13005/ojc/340510)
 47. Priolisi O, Fabrizi A, Deon G, et al. Morphology evolution of gold nanoparticles as function of time, temperature, and Au(III)/sodium ascorbate molar ratio. *J Nanoparticle Research* 2015; 18(1): 1. DOI: [10.1007/s11051-015-3308-7](https://doi.org/10.1007/s11051-015-3308-7)
 48. Anbu P, Gopinath SC, and Jayanthi S. Synthesis of gold nanoparticles using *Platycodon grandiflorum* extract and its antipathogenic activity under optimal conditions. *Nanomaterials Nanotechnology* 2020; 10: 1847980420961697.
 49. Aromal SA, Vidhu V, and Philip D. Green synthesis of well-dispersed gold nanoparticles using *Macrotyloma uniflorum*. *Spectrochimica Acta Part A: Molecular Biomolecular Spectroscopy* 2012; 85(1): 99–104.
 50. Doan V-D, Thieu AT, Nguyen T-D, et al. Biosynthesis of gold nanoparticles using *Litsea cubeba* fruit extract for catalytic reduction of 4-nitrophenol. *J Nanomaterials* 2020; 2020: 1–10.
 51. Princy K and Gopinath A. Optimization of physicochemical parameters in the biofabrication of gold nanoparticles using marine macroalgae *Padina tetrastratica* and its catalytic efficacy in the degradation of organic dyes. *J Nanostructure Chemistry* 2018; 8(3): 333–342.
 52. Singh AK and Srivastava ON. One-Step Green Synthesis of Gold Nanoparticles Using Black Cardamom and Effect of pH on Its Synthesis. *Nanoscale Research Letters* 2015; 10: 353. DOI: [10.1186/s11671-015-1055-4](https://doi.org/10.1186/s11671-015-1055-4)
 53. Wu SF, Yan SJ, Qi W, et al. Green synthesis of gold nanoparticles using aspartame and their catalytic activity for p-nitrophenol reduction. *Nanoscale Research Letters* 2015; 10: 213. DOI: [10.1186/s11671-015-0910-7](https://doi.org/10.1186/s11671-015-0910-7)
 54. Lim SH, Ahn E-Y, and Park Y. Green synthesis and catalytic activity of gold nanoparticles synthesized by *Artemisia capillaris* water extract. *Nanoscale Research Letters* 2016; 11(1): 1–11.
 55. Souza TG, Ciminelli VS, and Mohallem NDS. A comparison of TEM and DLS methods to characterize size distribution of ceramic nanoparticles. In: Paper presented at the Journal of physics: conference series, RS, Brazil, 2016.
 56. Zheng T, Bott S, and Huo Q. Techniques for accurate sizing of gold nanoparticles using dynamic light scattering with particular application to chemical and biological sensing based on aggregate formation. *ACS Applied Materials Interfaces* 2016; 8(33): 21585–21594.
 57. Ahn S, Singh P, Jang M, et al. Gold nanoflowers synthesized using *Acanthopanax cortex* extract inhibit inflammatory mediators in LPS-induced RAW264.7 macrophages via NF-kappa B and AP-1 pathways. *Colloids Surfaces B-Bio-interfaces* 2018; 162: 398–404. DOI: [10.1016/j.colsurfb.2017.11.037](https://doi.org/10.1016/j.colsurfb.2017.11.037)
 58. Yulizar Y, Utari T, Ariyanta HA, et al. Green Method for Synthesis of Gold Nanoparticles Using *Polyscias scutellaria* Leaf Extract under UV Light and Their Catalytic Activity to Reduce Methylene Blue. *J Nanomaterials* 2017; 2017: 3079636. DOI: [10.1155/2017/3079636](https://doi.org/10.1155/2017/3079636)
 59. Van Wyk BE. A review of commercially important African medicinal plants. *J Ethnopharmacology* 2015; 176: 118–134. DOI: [10.1016/j.jep.2015.10.031](https://doi.org/10.1016/j.jep.2015.10.031)
 60. Choi Y, Choi MJ, Cha SH, et al. Catechin-capped gold nanoparticles: green synthesis, characterization, and catalytic activity toward 4-nitrophenol reduction. *Nanoscale Research Letters* 2014; 9: 103. DOI: [10.1186/1556-276x-9-103](https://doi.org/10.1186/1556-276x-9-103)
 61. Hsieh DS, Wang H, Tan SW, et al. The treatment of bladder cancer in a mouse model by epigallocatechin-3-gallate-gold nanoparticles. *Biomaterials* 2011; 32(30): 7633–7640. DOI: [10.1016/j.biomaterials.2011.06.073](https://doi.org/10.1016/j.biomaterials.2011.06.073)
 62. Zhu S, Zhu L, Yu J, et al. Anti-osteoclastogenic effect of epigallocatechin gallate-functionalized gold nanoparticles in vitro and in vivo. *International Journal Nanomedicine* 2019; 14: 5017–5032.
 63. Baruah D, Goswami M, Yadav RNS, et al. Biogenic synthesis of gold nanoparticles and their application in photocatalytic degradation of toxic dyes. *J Photochem Photobiol B* 2018; 186: 51–58. DOI: [10.1016/j.jphotobiol.2018.07.002](https://doi.org/10.1016/j.jphotobiol.2018.07.002)
 64. Lee YJ, Cha SH, Lee KJ, et al. Plant Extract (*Bupleurum falcatum*) as a Green Factory for Biofabrication of Gold Nanoparticles. *Nat Prod Commun* 2015; 10(9): 1593–1596. Retrieved from <https://www.ncbi.nlm.nih.gov/pubmed/26594767>
 65. Lim SH, Ahn EY, and Park Y. Green synthesis and catalytic activity of gold nanoparticles synthesized by *artemisia capillaris* water extract. *Nanoscale Research Letters* 2016; 11(1): 474. DOI: [10.1186/s11671-016-1694-0](https://doi.org/10.1186/s11671-016-1694-0)
 66. Moustafa NE and Alomari AA. Green synthesis and bactericidal activities of isotropic and anisotropic spherical gold

- nanoparticles produced using *Peganum harmala* L leaf and seed extracts. *Biotechnol Appl Biochem* 2019; 66(4): 664–672. DOI: [10.1002/bab.1782](https://doi.org/10.1002/bab.1782)
67. Soshnikova V, Kim YJ, Singh P, et al. Cardamom fruits as a green resource for facile synthesis of gold and silver nanoparticles and their biological applications. *Artif Cells Nanomed Biotechnol* 2018; 46(1): 108–117. DOI: [10.1080/21691401.2017.1296849](https://doi.org/10.1080/21691401.2017.1296849)
68. Vijayan R, Joseph S, and Mathew B. Eco-friendly synthesis of silver and gold nanoparticles with enhanced antimicrobial, antioxidant, and catalytic activities. *Iet Nanobiotechnology* 2018; 12(6): 850–856. DOI: [10.1049/iet-nbt.2017.0311](https://doi.org/10.1049/iet-nbt.2017.0311)
69. Zayed MF and Eisa WH. Phoenix dactylifera L. leaf extract phytosynthesized gold nanoparticles; controlled synthesis and catalytic activity. *Spectrochim Acta A Mol Biomol Spectrosc* 2014; 121: 238–244. DOI: [10.1016/j.saa.2013.10.092](https://doi.org/10.1016/j.saa.2013.10.092)
70. Irfan M, Ahmad T, Moniruzzaman M, et al. Effect of pH on ionic liquid mediated synthesis of gold nanoparticle using *elaiseguineensis* (palm oil) kernel extract. In: Paper presented at the IOP Conference Series: Materials Science and Engineering, Bali, Indonesia, 2017.
71. Suvith V and Philip D. Catalytic degradation of methylene blue using biosynthesized gold and silver nanoparticles. *Spectrochimica Acta Part A: Molecular Biomolecular Spectroscopy* 2014; 118: 526–532.
72. Yulizar Y, Utari T, Ariyanta HA, et al. Green method for synthesis of gold nanoparticles using *Polyscias scutellaria* leaf extract under UV light and their catalytic activity to reduce methylene blue. *J Nanomaterials* 2017; 2017: 1–6.
73. Singh S. Nanomaterials Exhibiting Enzyme-Like Properties (Nanozymes): Current Advances and Future Perspectives. *Front Chem* 2019; 7: 46, DOI: [10.3389/fchem.2019.00046](https://doi.org/10.3389/fchem.2019.00046).
74. Noël S, Bricout H, Addad A, et al. Catalytic reduction of 4-nitrophenol with gold nanoparticles stabilized by large-ring cyclodextrins. *New J Chem* 2020; 44: 21007–21011.